Adama Science and Technology University

School of Applied Natural Science

Department of Chemistry

Final Research Report on

Synthesis and Luminescent Characteristics of

$(Ca_{4-x-y-z}Ba_ySr_z)(PO_4)_2O:xEu^{2+}$ Phosphors as a Potential Application

for White-Light Emitting Diode

by

Gemechu Deressa

January, 2018

Adama, Ethiopia

TABLE OF CONTENTS

LIST OF FIGURES

LIST OF TABLES

Synthesis and Luminescent Characteristics of $(Ca_{4-x-y-z}Ba_ySr_z)(PO_4)_2O:xEu^{2+}$ Phosphors' as a Potential Applications for White-Light Emitting Diode

Gemechu Deressa

Department of Chemistry, School of Applied Natural Science, Adama Science and Technology University, Adama, 1888, Ethiopia

ABSTRACT: *A novel tunable red- to yellow- emitting phosphor, $(Ca_{4-x-y-z}Ba_ySr_z)(PO_4)_2O:xEu^{2+}$ is reported that displays a broad emission from 500 to 800nm, and its emission can be adjusted from red to yellow by changing Ba^{2+} and Sr^{2+} doping concentration. X-ray powder diffraction analysis confirmed the phase formation. Excitation and emission spectra, and concentration dependence of emission intensity of the phosphor were investigated. The results showed that with increasing Ba^{2+}/Sr^{2+} concentration, the emission peak wavelength blue-shift from 594 to 567 nm, and the color can be tuned from red to yellow. When single- phase $(Ca_{2.95}Ba_{0.5}Sr_{0.5})(PO_4)_2O:0.05Eu^{2+}$ phosphor is pumped by a blue InGaN light-emitting diode we obtain white light with color rending index between 80.0 and 89.0 and color temperatures between 3500 and 5450 K, suggesting that this material is competitive as a color conversion material for solid state lighting.*

Keywords**:** *White light-emitting diode; Phosphors; Tunable emitting*

***** Corresponding Author: Gemechu Deressa, Mobile:,251911300993, E-mail Address: chemistryadama@gmail.com

1. INTRODUCTION

1.1.Background and Justification

Solid-state lighting (SSL) has received intense and growing interest over the past few years, due to light-emitting diodes (LEDs) properties of high luminous efficiency, long lifetimes, and low pollution and power consumption. It is a p–n junction diode that emits light when activated.[1] When a suitable voltage is applied to the leads, electrons are able to recombine with electron holes within the device, releasing energy in the form of photons. This effect is called electroluminescence, and the color of the light (corresponding to the energy of the photon) is determined by the energy band gap of the semiconductor. LEDs are typically small (less than 1 mm^2) and integrated optical components may be used to shape the radiation pattern.[2]

Appearing as practical electronic components in 1962, the earliest LEDs emitted low-intensity infrared light.[3] Infrared LEDs are still frequently used as transmitting elements in remote-control circuits, such as those in remote controls for a wide variety of consumer electronics. The first visible-light LEDs were also of low intensity and limited to red. Modern LEDs are available across the visible, ultraviolet, and infrared wavelengths, with very high brightness.

Early LEDs were often used as indicator lamps for electronic devices, replacing small incandescent bulbs. They were packaged into numeric readouts in the form of seven-segment displays and were commonly seen in digital clocks. Recent

developments have produced LEDs suitable for environmental and task lighting. LEDs have led to new displays and sensors, while their high switching rates are useful in advanced communications technology.

Light emitting diodes (LEDs) have many advantages over incandescent light sources, including lower energy consumption, longer lifetime, improved physical robustness, smaller size, and faster switching. Light-emitting diodes are used in applications as diverse as aviation lighting, automotive headlamps, advertising, general lighting, traffic signals, camera flashes, and lighted wallpaper. They are also significantly more energy efficient and, arguably, have fewer environmental concerns linked to their disposal.[4, 5]

The commercialized white light emitting diodes (WLEDs) can be generated by combining a blue-emitting InGaN-LED chip and a yellow-emitting garnet phosphor $Y_3Al_5O_{12}:Ce^{3+}$ ($YAG:Ce^{3+}$) [6-8]. However, such white light does not have sufficient color rendering properties. The color-rendering index (CRI) remains to be improved due to the lack of a full color component from the yellow phosphor. Recently, several WLED devices fabricated using ultraviolet (UV) chip coupled with a blend of tunable emitting (blue-to-yellow) and red-emitting phosphor, which exhibited favorable properties, including tunable correlated color temperature (CCT), tunable Commission International del'Eclairage (CIE) chromaticity coordinates, and excellent CRI values [8-13]. Unfortunately, the emission tunable range of the phosphor with a single activated ion has been reported is limited to blue to yellow.

The phosphors activated by rare-earth ions like; Ce^{3+} and Eu^{2+}, attract the attention of researchers due to the parity-allowed transitions between the 4f and 5d energy levels. The 5d state is an outer orbital; the energy associated with an electron in the 5d state depends strongly on the nature of the crystal field. Hence, the lanthanide 5d energy was vary remarkably. The absorption wavelengths of 4f orbital to 5d orbital transitions in Ce^{3+} and Eu^{2+} range from UV to red regions depending on a crystal-field splitting of the 5d levels, which is determined by the local structure of a host crystal [14, 15].

Changing the cation ratio of orthophosphate phosphate can distort the lattices structure due to change in crystal field of the host cases the broadening spectra of the luminescence are a promising hosts for lighting and display due to its good thermal stability and high luminescent efficiencies. The Eu^{2+}-activated Orthophosphate. Phosphates are good candidates as host structures and offer a number of merits, such as high chemical and low synthesis temperature and physical stability, and they exhibit interesting luminescence [16, 17].

The motivation of this work was to investigated a tunable red to yellow-emitting and efficient inorganic phosphors ($(Ca_{4-x-y-z}Ba_ySr_z)(PO_4)_2O:xEu^{2+}$) that could be applied in UV or blue LED-based solid state white light sources.

1.2. Statement of the Problem

Orthophosphate-phosphor doped with rare earth ions is widely explored as red, green and blue (RGB) phosphors owing to advantages of relatively low sintering temperature, good chemical stability, and satisfactory absorption in the ultraviolent (UV) to blue region [17-20]. $Ca_4(PO_4)_2O:Eu^{2+}$ is novel red-emitting phosphate phosphors [18]. To the best of our knowledge, its tunable emitting properties have not been reported in the literature. In this paper, we investigated a tunable red- to yellow- emitting $(Ca_{4-x-y-z}Ba_ySr_z)(PO_4)_2O:xEu^{2+}$ phosphor. This phosphor will be excited by light in UV to blue region and shows tunable red-to-yellow emission.

This paper reports the synthesis and luminescence properties of $(Ca_{4-x-y-z}Ba_ySr_z)(PO_4)_2O: xEu^{2+}$ phosphors based on the combination ratio of cations. The optical properties of Orthophosphate phosphate phosphors were systematically investigated by means of photoluminescence excitation (PLE) and emission (PL) spectra, thermal stability, Raman, and applications for white light emitting diodes (white-LEDs).

1.3. Objectives of the Study

- To Synthesis and characterizes the optical properties of (Ca, Sr, $Ba)_4(PO_4)_2O: Eu^{2+}$ phosphors.
- To improve the optical properties of white-LEDs
- To apply for high color rendering index white-LEDs,

1.4. Significance and Beneficiaries

- The Adama Sciences and Technology University is get information for research area on luminescent materials and LEDs.
- The project was develop a pilot scheme, the results of which were serve as a starting point for setting up an adequate system for application of LEDs.
- The project was also help to reduce the amount of hazardous and polluting emissions, thus improving air quality in Adama Town as well as in the country.
- The project can create job opportunity for the societies.
- The students build up their practical skills.
- The project collaborated with Pukyong National University, Department of Display Science and Engineering.

2. LITERATURE REVIEW

2.1. History of luminescence

Luminescence is a science related to spectroscopy. First Monades in 1565 extract luminescence from Librium nephiticiem, but it took until 1852 to be fully described by Sir G. G. Stokes who reported the theoretical basis for the mechanism of absorption (excitation) and emission. There are varied from of luminescence, is one of the fastest growing and most useful analytical tools in science. Applications can be found in areas as varied as environmental science, materials science, chemistry, microelectronics, physics, biology, biochemistry, medicine, pharmaceuticals, toxicology, and clinical chemistry. This dramatically changed has occurred only in the past couple of decades and has been principally driven by the unique needs of the life sciences [21-24].

The term ‘Luminescence’ was first used in 1888 by German physicist and historian of science Eilhardt Wiedemann. He defined luminescence as ‘all those phenomena of light which are not solely conditioned by the rise in temperature’. Wiedemann interpreted luminescence as the contrast of incandescence where luminescence refers to cold light and incandescence refers to hot light. A luminescing system is constantly expending energy to drive the emission process. The general term luminescence includes a wide variety of light emitting processes which derive their names from the varied sources of energy that power them. Photoluminescence, which includes phosphorescence and fluorescence, is one among many luminescent

categories [25, 26]. To illustrate the diversity of luminescence emissions, the following represent some of the more commonly observed types of luminescence:

1. ***Electroluminescence*** is produced by the passage of an electric current through an ionized gas. Example:- a gas discharge lamp.
2. ***Radioluminescence*** obtains its energy from the high energy particles released via radioactive decay. Example:- a luminous radium watch dial.
3. ***Triboluminescence*** is derived from the Greek word tribo meaning to rub. It is emitted when certain crystals are stressed, crushed, or broken. Example:- certain types of sugar crystals.
4. ***Sonoluminescence*** is produced in liquids exposed to intense sound (compression) waves.
5. ***Chemiluminescence*** derives its energy from chemical reactions. It is the breaking of chemical bonds that supplies the energy.
6. ***Bioluminescence*** can be considered a subdivision of chemiluminescence. It occurs when chemiluminescent reactions take place in living systems and usually involves ATP reaction. Example:- light emitted by fireflies and glow-worms.
7. ***Cathodoluminescence*** is light that is generated from the exposure of substances to cathode rays.
8. ***Photoluminescence***

Photoluminescence occurs when a system is excited to a higher energy level by absorbing a photon, and then spontaneously decays to a lower energy level, emitting a photon in the process. To conserve energy, the emitted photon cannot have more energy than the exciting photon, unless two or more excitation photons act in

tandem. Intermediate nonradiative downward transitions are possible. The electron can also be stored in an intermediate state for a long time, resulting in delayed luminescence.

Photoluminescence is divided into three types, depending upon the nature of the ground and the excited states. In a singlet excited state, the electron in the higher-energy orbital has the opposite spin orientation as the second electron in the lower orbital. These two electrons are said to be paired. In a triplet state these electrons are unpaired, that is, their spins have the same orientation. Return to the ground state from an excited singlet state does not require an electron to change its spin orientation. A change of spin orientation is needed for a triplet state to return to the singlet ground state Figure 2.1. **Fluorescence** is the emission which results from the return to the lower orbital of the paired electron. Such transitions are quantum mechanically "allowed" and the emissive rates are typically near 10^{-8} s^{-1}. These high emissive rates result in fluorescence life times near 10^{-8} s or 10 ns. The lifetime is the average period of time a fluorophore remains in the excited state. **Phosphorescence** is the emission which results from transition between states of different multiplicity, generally a triplet excited state returning to a singlet ground state. Such transitions are not allowed and the emissive rates are slow. Typical phosphorescent lifetimes range from milliseconds to seconds, depending primarily upon the importance of deactivation processes other than emission. **Delayed fluorescence** is a rare phenomenon whereby the electron responsible for the emission starts out in the singlet state, crosses over to the triplet state, but eventually

returns to the singlet state prior to emission. The result is a singlet state emission of much longer lifetime than normal [27, 28].

2.2. Luminescent Materials for LEDs

The next revolution in general lighting was marked by the invention of the fluorescent lamp. Important inventive steps were disclosed in [29], the first commercially viable product was invented by GE, in 1936 [30]. Initially, this concept was thought to be very suitable for colored advertisement lamps, especially blue light could be generated with much higher efficacy than by filtering blue light out of the light generated by incandescent lamps. Very soon afterwards, the potential of this concept to generate white light became very clear and already before the Second World War, fluorescent lamps were in use. Fluorescent lamps do not generate as much IR radiation as incandescent lamps, for this reason their efficacy is much higher than that of incandescent lamps. In the 1970-ies, after the invention of rare-earth based luminescent materials, a significant further increase in efficacy was realized. Again, the dependence of the eye-sensitivity on the photon wavelength played an important role. Most of the luminescent materials applied in fluorescent lamps before the advent of rare-earth phosphors show broad emission spectra, f.e., spectra with a FWHM of 50–100 nm. To generate white light with a high color rendering index (the ability to reproduce all colors in a natural way), blue, green and red light have to be present in the emission spectrum of the lamps, with maxima at about 450 nm, 550 nm and 600 nm, see Figure 2. 1. In this Figure, the CIE's (Commission Internationale de l'Eclairage) color matching functions are numerical descriptions of the chromatic response of the human eye; the green curve gives the

overall eye sensitivity. Especially in the red part of the spectrum, the eye sensitivity decreases strongly above 600 nm and for this reason broad emission spectra in the red part of the spectrum lead to a significant loss in lumen output, even though the quantum efficiencies of the luminescent material applied to generate red light may be very high [29, 30].

2.3. Phosphor Materials

The luminescent materials known as, phosphors convert energy into electromagnetic radiation, usually in the visible energy range. Phosphors are solid luminescent materials that emit photons when excited by an external energy source. Luminescence continues to play a major technological role for mankind. Solid-state luminescence is now set to significantly displace gas discharge luminescence in many areas, in much the same way as gas discharges have already displaced tungsten filament incandescence.

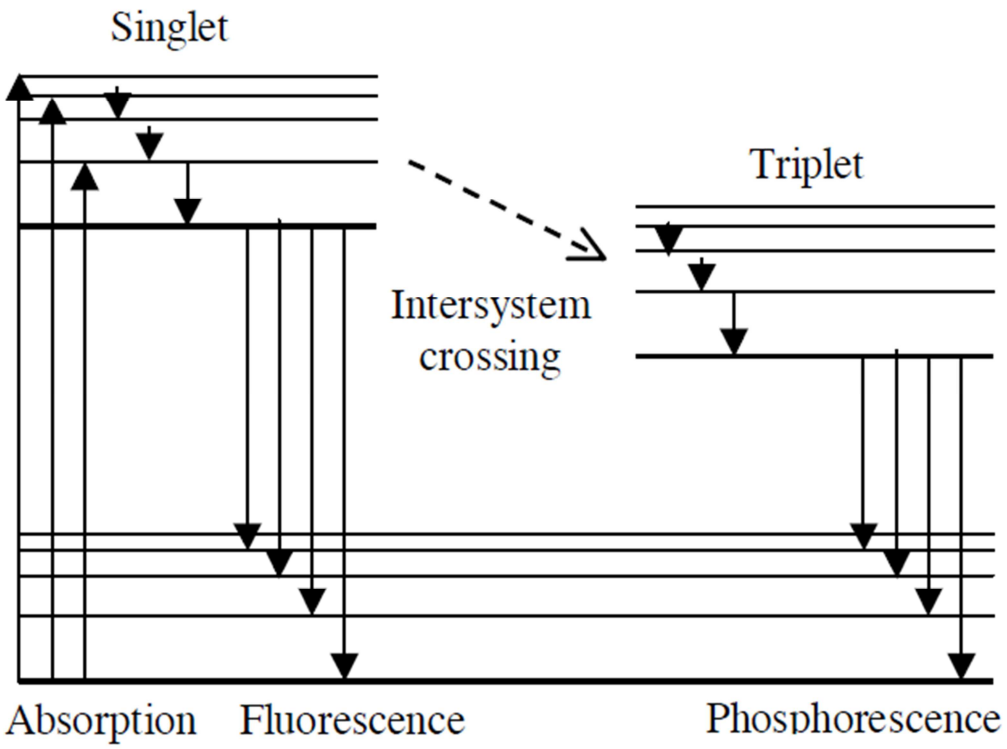

Figure 2. 1 Fluorescence and phosphorescence mechanism

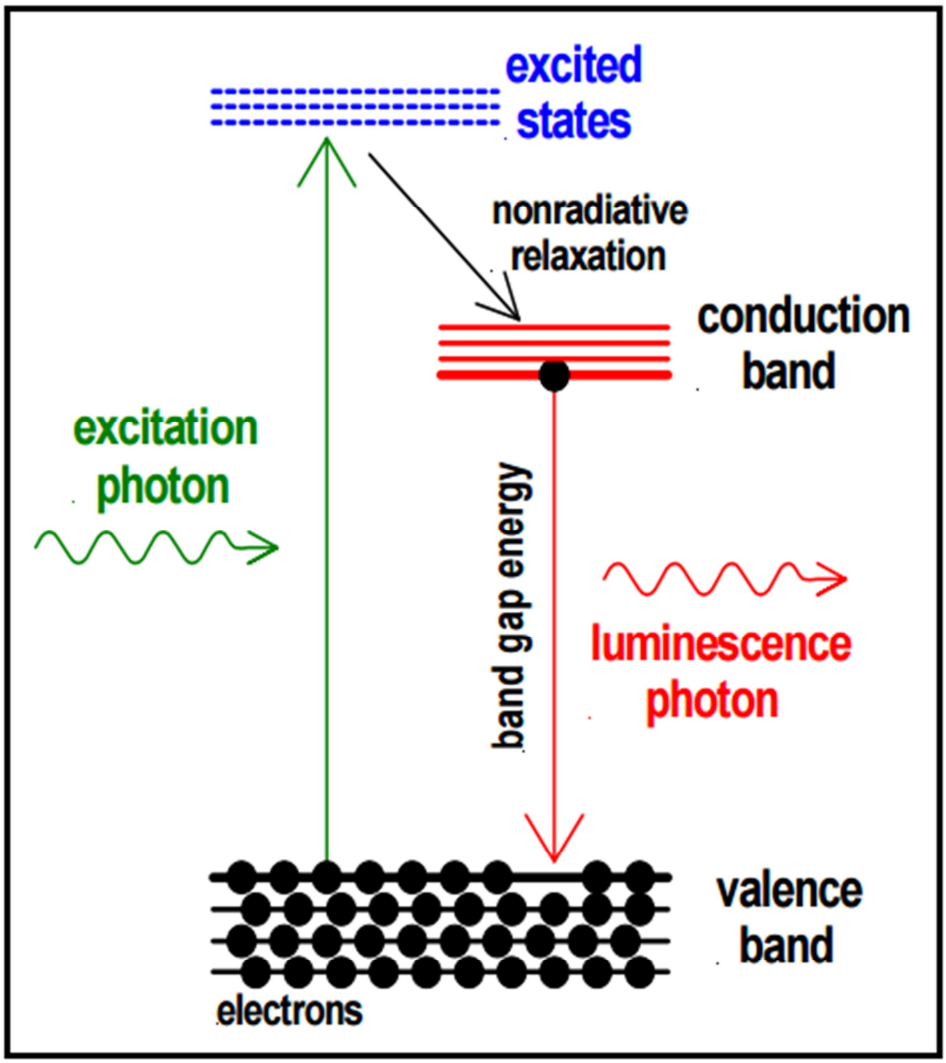

Figure 2. 2 Basic Principle of luminescence

All solids, including semiconductors, have energy gaps for the conducting electrons. In order to understand the concept of a gap in energy, first consider that some of the electrons in a solid are not firmly attached to the atoms, as they are for single atoms, but can hop from one atom to another. These loosely attached electrons are bound in the solid by differing amounts and thus have much different energy. Electrons having energies above a certain value are referred to as conduction electrons, while electrons having energies below a certain value are referred to as valence electrons. This is shown in the diagram where they are labeled as conduction and valence bands. The word band is used because the electrons have a multiplicity of energies in either band Figure 2.2. Furthermore, there is an energy gap between the conduction and valence electron states. Under normal conditions electrons are forbidden to have energies between the valence and conduction bands [31-35].

If a light particle (photon) has energy greater than the band gap energy, then it can be absorbed and thereby raise an electron from the valence band up to the conduction band across the forbidden energy gap. In this process of photo-excitation, the electron generally has excess energy which it loses before coming to rest at the lowest energy in the conduction band. At this point the electron eventually falls back down to the valence band. As it falls down, the energy it loses is converted back into a luminescent photon which is emitted from the material. Thus the energy of the emitted photon is a direct measure of the band gap energy, Eg. The process of photon excitation followed by photon emission is called

photoluminescence. Luminescent compounds are of very different kinds. Some of them can be listed as follows:

a) Organic compounds: Aromatic hydrocarbons, coumarins, polyenes. oxazines, fluorescein, amino acids, etc.

b) Inorganic compounds: Uranyl ion (UO^{2+}), lanthanide ions, glasses with Nd,Mn, Ce, Sn, Cu, Ag, etc, crystals like ZnSe ZnS, CdS, CdSe, GaS, GaP, Al_2O_3, etc.

c) Organometallic compounds: Lanthanide ion complexes, Ruthenium complexes, complexes with fluorogenic chelating agents like 8-hydroxyquinoline, etc.

2.4. Emission and Excitation Mechanisms of Phosphors

Luminescence phenomenon takes place in several steps. First, the energy of excitation is absorbed. This absorption can actually either correspond to the transition of an electron from the valence band to the conduction band of the host lattice (Absorption over the band gap), or to the transfer of a charge from a ligand to the optical center (Charge-transfer absorption), or also to the promotion of an electron of the activator from a certain energy level to another, within its orbitals. The absorbed energy may finally transfer to the activator, which goes from a ground state, to an excited state. During the return to the fundamental state, energy can be released in a radiative way, which is responsible for the observed luminescence properties [31, 33].

The overall phenomenon of absorption-emission by an activator is often described by a configurational coordinate diagram (Figure 2. 3): it represents the potential energy curves of the different energy levels of a luminescent center as a function of a configurational coordinate. If one considers that the central ion is immobile while the ligands around it are moving in phase, the configurational coordinate can be written as R, which varies proportionally to the metal-ligand distance. The resulting curve has a parabolic shape, because in the approximation of a harmonic vibrational motion, the problem is equivalent to a harmonic oscillator: $E = \frac{1}{2}k(R - R_0)^2$, R_o is the position of lowest energy, *i.e.* the equilibrium position. Quantum mechanics indicates that the system can take only discrete values in the potential curve, corresponding to some frequencies of the oscillator: $E_v = \left(V + \frac{1}{2}\right)\hbar\omega$ with V = 0, 1, 2 and ω is the frequency of the oscillator. This frequency can change between the ground and the excited state. The force constant k of the parabolas changes in consequence [32].

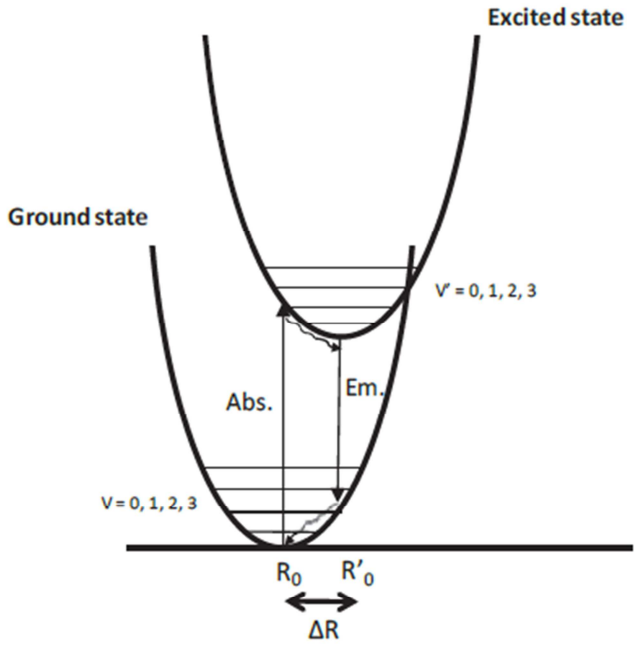

Figure 2. 3 Configurationally coordinate diagram illustrating the absorption-relaxation emission cycle [32].

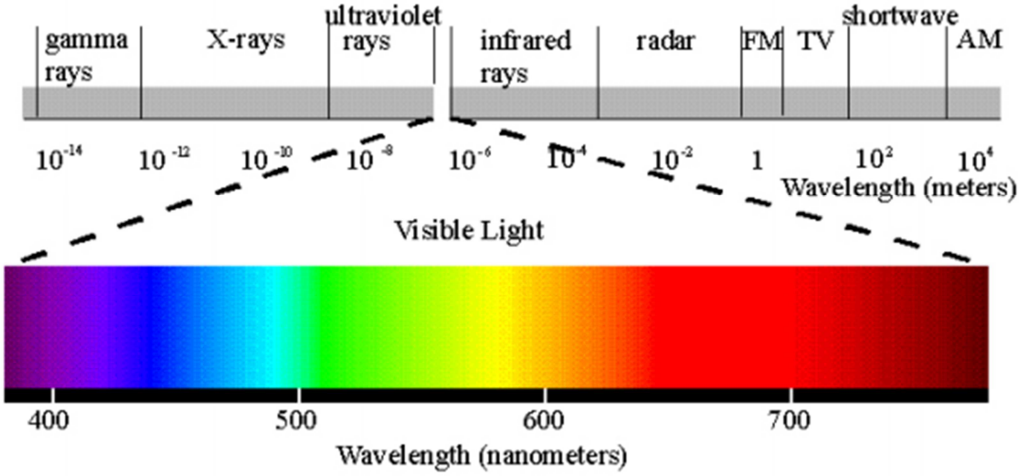

Figure 2. 1 The electromagnetic spectrum with the visible light region blown up [33]

The electromagnetic spectrum, shown in Figure. 2. 4, covers a huge range of wavelengths, from gamma rays at 10^{-14} m to AM radio waves at 10^{4} m. In this lab we are going to be concerned with the narrow band of wavelengths, ~ 400 – 750 nm (a nm = 10^{-9} m), that make up visible light. In order to know very accurately what wavelengths are being emitted by a source of light, we will use a digital spectrometer. Excitation and emission spectra of phosphors can be measured by spectrophotometers. An emission spectrum is the wavelength distribution of an emission measured at a single constant excitation wavelength. Conversely, an excitation spectrum is the dependence of emission intensity, measured at a single emission wavelength, upon scanning the excitation wavelength. Such spectra can be presented on either a wavelength scale or a wavenumber scale. Light of a given energy can be described in terms of its wavelength λ, frequency ν, or wavenumber.

The past few decades have seen spectacular developments in research on luminescence. There has been phenomenal growth in the subject and significant progress has been made. Rare earth ion-activated phosphors have numerous applications in the display, lighting, and medical industries. In recent years, the luminescent properties of phosphate materials have been widely investigated for their many advantages, such as excellent thermal and chemical stability, and the development of optical devices based on rare earth (RE) ion-doped materials has proven to be one of the most interesting fields of research. In this context, phosphates are investigated because of their low cost, their high stability for use in lamp applications, and their important crystallographic possibilities with regard to the accommodation of luminescent ions for in detail read [32-35].

The material Y_2O_3:Eu (applied widely in fluorescent lamps) shows almost monochromatic emission at 610 nm, without a long tail in the extended red part of the visible spectrum. Nowadays fluorescent lamps can have efficacies of up to some 100 lm/W, i.e., 10 times higher than incandescent lamps. Despite this very significant increase in efficacy, the energy efficiency of fluorescent lamps is still rather low. This is due to the fact that the spectrum emitted by the low pressure Hg-discharge that is operating in fluorescent lamps consists mainly of photons with wavelength 185 nm and 254 nm. To generate visible light, these photons have to be down converted to photons with significantly smaller photon energies. Together with the discharge efficiency of 70%, the resulting overall efficiency of fluorescent lamps is only some 25%. Compact fluorescent lamps have even lower efficiencies: 15%. Looking at the wavelengths, based on energy conservation it would be

possible to generate two photons in the green and red part of the spectrum (or even one blue photon and a red photon) after absorption of one UV photon originating from the Hg-discharge (quantum cutting). Indeed, there has been extensive research into this direction. Systems have been found with quantum efficiencies clearly exceeding 100%, based on cascade emission on Pr^{3+} [36, 37] and also in ion pairs [38, 39]. In the case of Pr^{3+}, one of the photons generated has a wavelength of 408 nm, which is too short for high color rendering and attempts to transfer this energy to ions like Mn^{2+} or Cr^{3+} to obtain more useful photons have failed for reasons not understood yet. The other photon generated in the cascade has a wavelength of about 615 nm, i.e., very suitable for application in light sources with good color rendering and high lumen output.

The next revolution in lighting is now going on. Inorganic and organic LEDs, operated at low voltage generate light by recombination of electron and holes.

3. EXPERIMENTAL PROCEDURE

Materials: Appropriate amounts of starting materials, calcium carbonate $CaCO_3$ (99.99%) barium carbonate $BaCO_3$ (99.99%) and strontium carbonate $SrCO_3$ (99.99%), Ammonium hydrogen phosphate $(NH_4)_2HPO_4$ (99.0%), ammonium chloride (NH_4Cl) and europium oxide Eu_2O_3 (99.99%) were purchased from Addisa Ababa chemcal shops and all are Sigma Aldrich except ammonium chloride. The exapermantal activeties esptialy the solid state reactions are preformed at Adama Science and Technology University, School of Appleid Natural Science, Department of Applied Chemistry and the charactarization of as synthesized samples were performed at Pukyong National University, Department of Display Science and Engineering.

3.1.Preparation $(Ca_{4-x-y-z}Ba_ySr_z)(PO_4)_2O:xEu^{2+}$ phosphate phosphors

Powder samples of Orthophosphate phosphors were prepared by a solid-state reaction. MCO_3 (99.99%), [M = Ca, Sr and Ba], $(NH_4)_2HPO_4$ (99.0%), and Eu_2O_3 (99.99%) are weighed, thoroughly mixing and ground in an agate mortar. The mixed powders were then transferred into an alumina crucible, and pre-sintered in a furnace at 500 ℃ for 2 hours in air to eliminate the water and decompose the carbonate. The pre-sintered samples were subsequently cooled down to room temperature and fully ground to form a homogeneous mixture. Then the mixture was re-sintered at a high temperature of 1000 to 1300 ℃ for 4 hours under a reducing atmosphere ($5\%H_2/95\%N_2$) for 4 hours After sintering, the samples were cooled

down naturally to room temperature in the furnace. The acquired sintered products were pulverized for further measurements. The nominal molar compositions of the phosphors are as follows: $Ca_{4-x-y}Ba_ySr_z(PO_4)_2O:_XEu^{2+}$ ($0.01 \leq X \leq 0.10$, $0 \leq Y \leq 2.5$, and $0 \leq Z \leq 2.5$) [9].

3.2 Materials Characterization

The as-prepared samples were characterized by using the following instruments; Scanning electron microscope (SEM: LEO SUPRA 55, Carl Zeiss) attached with an energy dispersive X-ray spectrometer (EDX), X-ray diffractometer (M18XHF-SRA, Mac Science), X-ray diffraction (XRD) analysis using a Rigaku D/MAX 2500 with Cu Kα radiation. The measurements of photoluminescence (PL) and photoluminescence excitation (PLE) spectra are carried out using a DARSA PRO-5200 fluorescence spectrophotometer equipped with a xenon lamp as the excitation light source. The thermal quenching characteristics are measured in the temperature range of 25-200 ℃. Raman spectra of (Ca, Sr, $Ba)_4(PO_4)_2O$: Eu^{2+} are carried out at room temperature in the range of 200 to 2000 cm^{-1} using Agiltron, Raman Spectrometer, which is having excitation Nd:YAG laser) a excitation laser source (1064 nm).

3.3 LED Lamp Fabrication.

The WLEDs were fabricated using a blue-LED chip with a 450 nm excitation wavelength. First of all, the chip was assembled on a LED frame and care was taken

to prevent the formation of air bubbles between the chip and frame, because it can damage the LED when a forward bias current was applied. The semi-transparent silicone epoxy was prepared by mixing two optical encapsulants, i.e., OE-6630 A (base) and OE-6630 B (catalyst) in 1:2 ratio. Afterwards, the required quantity of $(Ca_{2.95}Ba_{0.50}Sr_{0.50}Eu_{0.05})(PO_4)_2O$ phosphor powders were mixed with the silicone epoxy, kept in a mixer and later kept in a desiccator to remove the air bubbles. Finally, it was poured in a dispenser tube. The phosphor mixed epoxy was later dispensed onto the LED frame and kept in an oven (@ 120 °C, for 90 min) to harden, and eventually the WLEDs were characterized by using an OL770 multi-channel spectroradiometer attached with an integrating sphere.

4. RESULTS AND DISCUSSION

4.1 Phosphor Synthesis and Characterization.

Figure 4. 1 shows the results of the data collection and structure refinements for $(Ca_{2.95}Ba_{0.50}Sr_{0.50}Eu_{0.05})(PO_4)_2O$. The single crystal structure data of $Ca_4(PO_4)_2O$ (ICSD no. 2631) was performed as starting reference to approach the actual crystal structure. The final converged weighted-profile of R_{exp}=6.99, R_{wp}= 9.16, R_p=7.09 and *GOF*=1.31 is shown in Table 1. The $(Ca_{2.95}Ba_{0.50}Sr_{0.50}Eu_{0.05})(PO_4)_2O$ crystallizes in a monoclinic unit cell with space group P21(4) space group with Z = 4. In the crystal structure of $Ca_4(PO_4)_2O$, the Ca^{2+} ions have eight different coordination environments, only Ca(6) ion is eight-coordinated, and the other Ca^{2+} ions are seven-coordinated (See Figure 4.1 (b)).

Table 4. 1 Rietveld refinement and crystal data of Rietveld enhancement and crystal data of $(Ca_{2.95}Ba_{0.50}Sr_{0.50}Eu_{0.05})(PO_4)_2O$ phosphors.

Formula	$Ca_{3.95}(PO_4)_2O:0.05Eu^{2+}$
Cryst. syst.	$P2_1(4)$ – monoclinic
Crystal Density (g/cm^3)	7.229
Units, Z	4
a (Å)	7.012 (11)
b (Å)	11.979 (13)
c (Å)	9.481 (9)
V ($Å^3$)	797.32576(15)
β (deg)	90.6(2)
R_{exp} (%)	6.89
R_{wp} (%)	9.14
R_p (%)	7.06
GOF	1.29

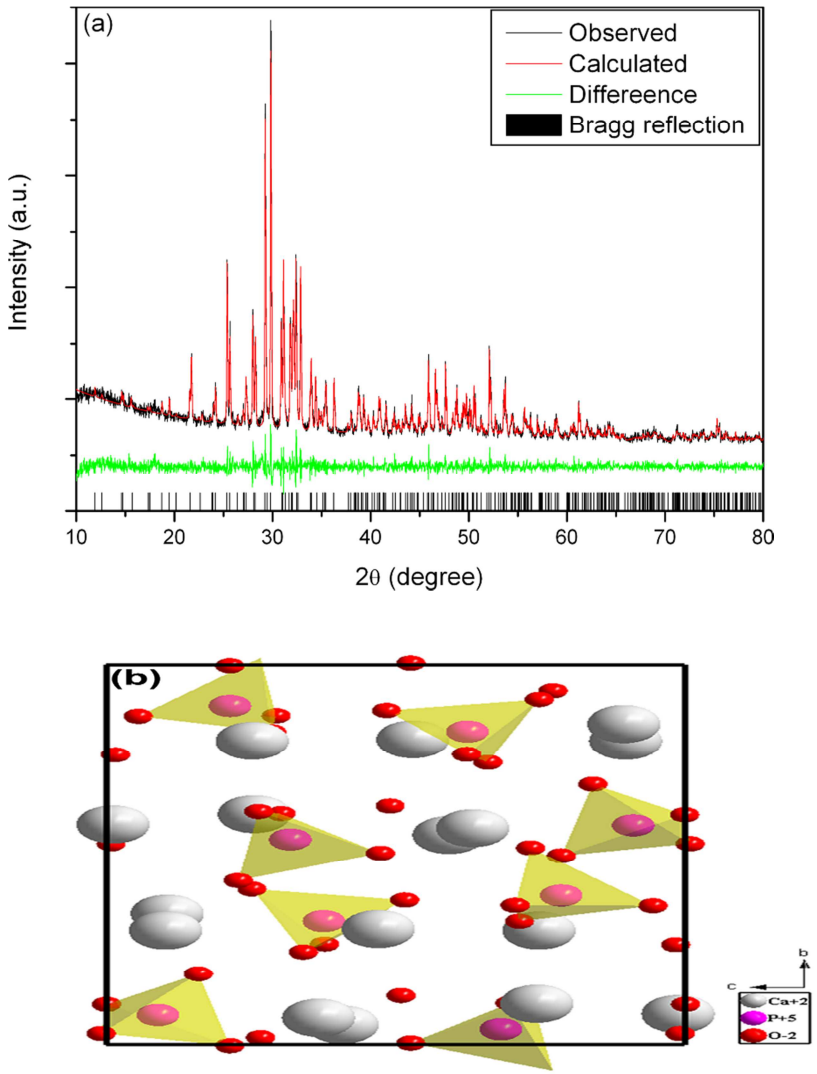

Figure 4. 1(a) Observed (black), calculated (red), and difference (green) synchrotron XRD profiles for the Rietveld refinement of $(Ca_{2.85}Ba_{0.50}Sr_{0.50})(PO_4)_2O{:}0.05Eu^{2+}$. Bragg reflections are indicated with tick marks. (b) Crystal structure of $Ca_4(PO_4)_2O$ unit cell viewed in a-direction (Ref. 19).

The XRD patterns of $(Ca_{4-y-z}Ba_ySr_z)(PO_4)_2O:0.05Eu^{2+}$ together with the Joint Committee on Powder Diffraction Standards (JCPDS) card No. 73-1379 are shown in Figure 4. 2. When the Sr^{2+} doping content (z), the diffraction peaks of the obtained sample can be indexed to the standard data except for little shift, indicating that these samples almost are single-phase. When the Ba^{2+} doping content (y), the diffraction peaks of the obtained sample can be indexed to the standard data except for little shift, indicating that these samples almost are single-phase. $Eu^{2+}/Ba^{2+}/Sr^{2+}$ are incorporated in the host lattice [16].

When the Ba^{2+} doping content (*y*) is higher than 0.10, The intensity of some crystal planes diffraction peak increased gradually, such as (200), (210) and (212), which indicated that with the increase of Ba^{2+} ions substituted, resulting in corresponding crystal face preferred growth. Additionally, the diffraction peaks exhibit a shift toward smaller angles with rising doping content of the Ba^{2+} ion, which may be related to the substitution of smaller Ca^{2+} by the lager Ba^{2+}.

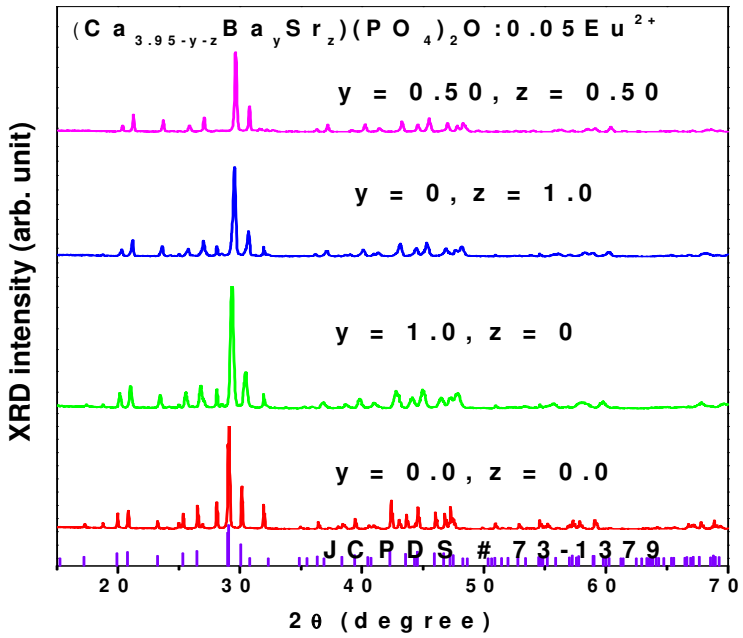

Figure 4. 2 XRD patterns of $(Ca_{4-y-z}Ba_ySr_z)(PO_4)_2O:0.05Eu^{2+}$ phosphors

The micromorphology of the crystalline $(Ca_{2.95}Ba_{0.50}Sr_{0.50}Eu_{0.05})(PO_4)_2O$ phosphor sample observed by SEM is shown in Figure 4. 3. It is observed that the particles have smooth morphology and the diameters are ranging from 15 to 20 μm. The elemental composition of $(Ca_{2.95}Ba_{0.50}Sr_{0.50}Eu_{0.05})(PO_4)_2O$ sample verified by EDS shows (wt %) Ca 35.28%, Ba 3.23%, Sr 3.38, Eu 2.25 %, P 16.34 % and O 38.91%. The composition suggested by EDS is consistent with stoichiometric weight ratio with reasonable relative error.

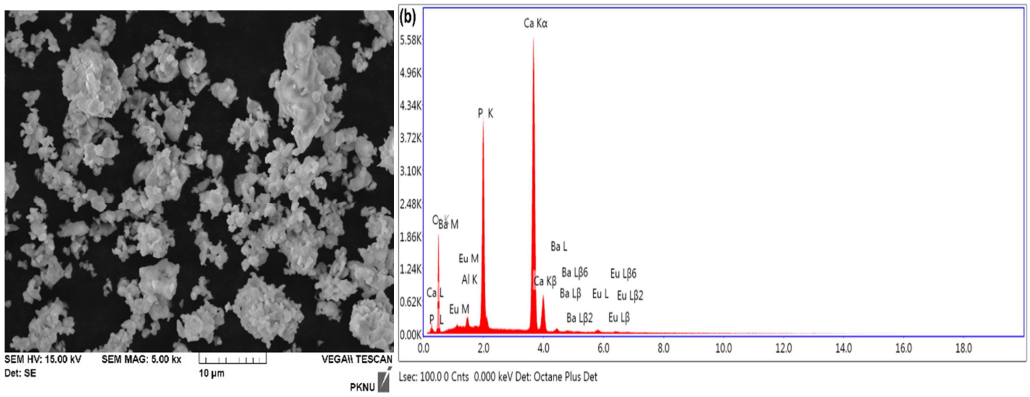

Figure 4. 3 (a)SEM image and (b) EDS profile of $(Ca_{2.95}Ba_{0.50}\,Sr_{0.50}Eu_{0.05})(PO_4)_2O$ sample

The Raman spectra of as synthesized $(Ca_{4-y-z}Ba_ySr_z)(PO_4)_2O{:}0.05Eu^{2+}$ phosphors in the 200 to 2000 cm^{-1} region are shown in Figure 4. 4. The results of the band component analyses of the Raman spectra are reported in Table 2. The Raman spectra show intense bands in the 920 to 950 cm^{-1} region [7, 8]. A single intense band is observed for the samples at 949.544, 942.289, 934.849, and 941.308 cm^{-1},

$(Ca_{2.95}Ba)(PO_4)_2O:0.05Eu^{2+}$, $(Ca_{2.95}Sr)(PO_4)_2O:0.05Eu^{2+}$ and $(Ca_{2.95}Ba_{0.50}\ Sr_{0.50})(PO_4)_2O:0.05Eu^{2+}$and undoped host $Ca_{3.95}(PO_4)_2O:0.05Eu^{2+}$, respectively. These bands are distorted based on the cation sizes attached to the PO_4 ligands and also due to Eu^{2+} doped. $(Ca_{2.95}Ba)(PO_4)_2O:0.05Eu^{2+}$, $(Ca_{2.95}Sr)(PO_4)_2O:0.05Eu^{2+}$, The Raman vibrational frequencies decrease by 15.003 cm^{-1} upon substitution of Ba^{2+}/Sr^{2+} for Ca^{2+} and decrease by 6.422 cm^{-1} when one mole of of Ca^{2+} substituted by Ba^{2+}/Sr^{2+} in the lattices due to size of Ba^{2+}/Sr^{2+} greater than size of Ca^{2+} ions. In the same way, the Raman vibration frequencies of Eu^{2+} doped $(Ca_{2.95}Ba_{0.50}Sr_{0.50})(PO_4)_2O:0.05Eu^{2+}$ higher by 2.143 cm^{-1} than undoped $Ca_{3.95}(PO_4)_2O:0.05Eu^{2+}$lattices.

The Raman vibrational frequencies of v_2, v_3, and v_4 are follows the same phenomenal. The shift in the observed Raman frequencies is believed to be due a tightening or enlargement of the molecular PO_4^{3-} ion as oxygen atoms of neighboring molecules are either drawn near or pushed apart on substitution of cations of different size. The bond length of Ba-O/ Sr-O are longer than the C-O in the crystal structure of $Ba_4PO_4)_2O$, $Sr_4PO_4)_2O$ and $Ca_4PO_4)_2O$, respectively. The crystal structure of $(Ca_{2.95}Ba_{0.50}Sr_{0.50})(PO_4)_2O:0.05Eu^{2+}$ formed from mixed crystal structure of $Ba_4PO_4)_2O$, $Sr_4PO_4)_2O$ and $Ca_4PO_4)_2O$ as observed from XRD and Raman properties of the structures, Both XRD and Raman spectra of the host $(Ca_{2.95}Ba_{0.50}Sr_{0.50})(PO_4)_2O$ found between these three hosts of $Ba_5(PO_4)_3Cl$ and $Sr_5(PO_4)_3Cl$ lattices. This indicate that the lattices of $(Ca_{2.95}Ba_{0.50}Sr_{0.50})(PO_4)_2O$ host combined from an expanded Ba-O/Sr-O and contracted Ca-O bonds which create different environments around the sites of Eu^{2+} ions doped in the lattice of

$(Ca_{2.95}Ba_{0.50}Sr_{0.50})(PO_4)_2O$ phosphor and cause for the blue shifts and spectral broadening of Eu^{2+} activated $(Ca_{2.95}Ba_{0.50}Sr_{0.50})(PO_4)_2O$ phosphors[9, 10].

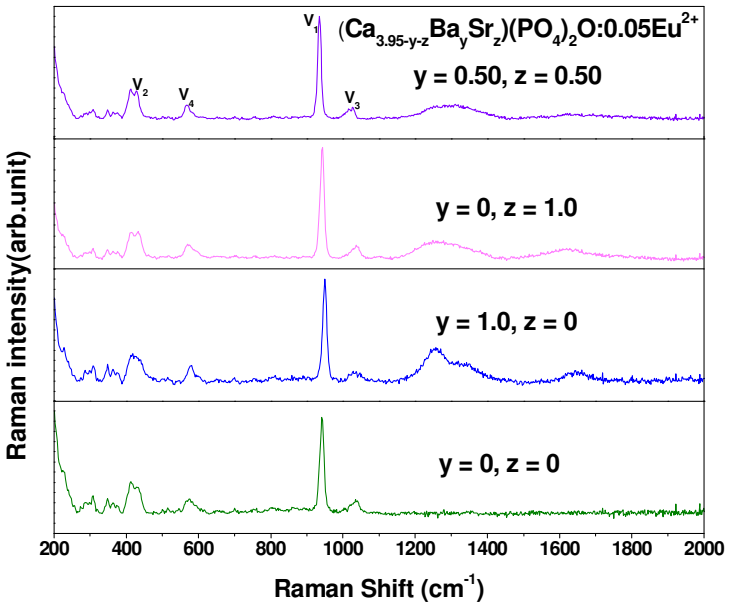

Figure 4. 4 . Raman spectra of the $(Ca_{4-y-z}Ba_ySr_z)(PO_4)_2O:0.05Eu^{2+}$ phosphors

Table 4. 2. Raman shifts of PO_4 modes in $(Ca_{3.95-y-z}Ba_ySr_z)(PO_4)_2O:0.05Eu^{2+}$

No	Phosphors	V_1	V_2	V_3	V_4	Reference
1	$(Ca_{3.95-}(PO_4)_2O:0.05Eu^{2+}$	941.308	415.376 432.548	1040.699	574.428	This work
2	$(Ca_{2.95}Ba)(PO_4)_2O:0.05Eu^{2+}$	949.873	417.834 456.954	1028.162	581.508	This work
3	$(Ca_{2.95}Sr)(PO_4)_2O:0.05Eu^{2+}$	934.870	412.917 427.649	1026.068	567.335	This work
4	$(Ca_{2.95}Ba_{0.50}Sr_{0.50})(PO_4)_2O:0.05Eu^{2+}$	943.451	415.376 432.548	1036.525	569.701	This work
5	$[PO_4]^{3-}$	938	420	1017	567	Ref. 19

4.2 Excitation and Emission Properties of $(Ca_{3.95-y-z}Ba_ySr_z)(PO_4)_2O:0.05Eu^{2+}$.

The excitation and emission spectrum of $(Ca_{2.95}Ba_{0.50}Sr_{0.50})(PO_4)_2O:0.05Eu^{2+}$ are shown in Figure 4. 5. Under 450 nm excitation, there are the broad asymmetric emission spectrum peaking at 567 nm with four broad emission bands centered at 567, 608, 632 and 667 nm, respectively. The broad emission shows that Eu^{2+} has more than one emission center in $Ca_4(PO_4)_2O$ which belongs to the typical emission of Eu^{2+} ions ascribed to 5d→4f transitions. By Gaussian deconvolution, the emission spectrum of $(Ca_{2.95}Ba_{0.50}Sr_{0.50})(PO_4)_2O:0.05Eu^{2+}$ can be well-decomposed into eight Gaussian proflies peaking at 534 nm, 556 nm, 567 nm, 592, 608 nm, 632 nm, 667 nm, 673 nm and 674nm, which can be ascribed to eight different Ca^{2+} sites occupied by Eu^{2+} ions. The refinement shows that the structure of $Ca_4(PO_4)_2O$ contains eight crystallographically distinct Ca^{2+} sites that can be occupied by Eu^{2+}. The Eu^{2+} ions substituting Ca^{2+} ions in the site which has shorter Ca-O band distance are expected to experience stronger crystal field strength corresponding to a longer wavelength emission with larger Stoke shift, when the crystal environments are analogous. Figure 4. 5 illustrates eight kinds of cations ions coordinated with oxygen atoms, corresponding to the eight Gaussian profiles in the emission spectrum [7-11].

It is also observed that the excitation spectrum monitoring by 594 nm exhibits a different spectral profile, which means that the Ba/Sr substitute Ca at diferent site in the lattics and emission bands should be ascribed to different sites occupied by Eu^{2+} ions, which is also in accordance with the above analysis on the crystal structure.

The excitation spectrum shows a broad absorption from 300 to 500 nm with different maximum in the range, which corresponds to the $4f^7 \rightarrow 4f6^5d^1$ transition of th e Eu^{2+} ions. $(Ca_{3.95-y-z}Ba_ySr_z)(PO_4)_2O:0.05Eu^{2+}$ can be efficiently excited by blue light (350~480 nm), which is very advantageous for application in the W-LEDs

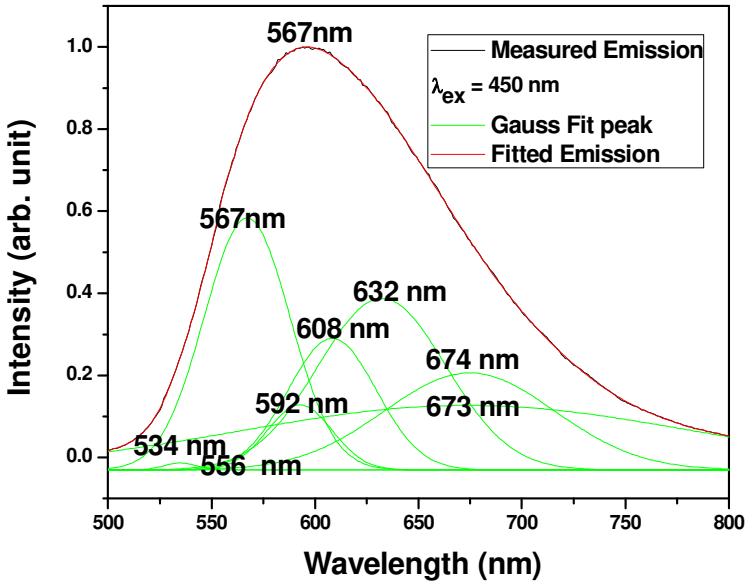

combined with highly efficient blue-InGaN chips (Figure 4. 5b) [13-17].

Figure 4. 5 Emission specra of $(Ca_{2.95}Ba_{0.50}Sr_{0.50})(PO_4)_2O:0.05Eu^{2+}$ (λ_{ex} = 450nm) measured emission (black line), fitted curve (red line) and deconvoluted Gaussian curve

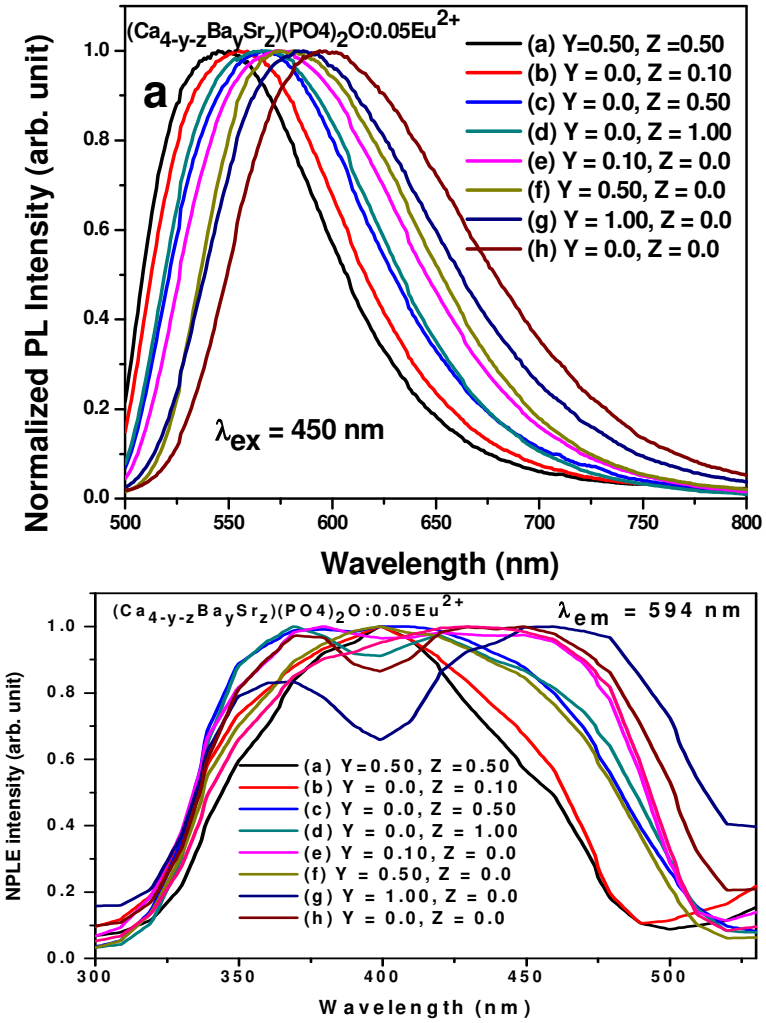

Figure 4. 6 (a) Emission spectra (λ_{ex} = 450nm) and, (b) Excitation (λ_{em} = 594) of $(Ca_{3.95-y-z}Ba_ySr_z)(PO_4)_2O$: $0.05Eu^{2+}$,).

Figure 4. 6(a) shows room temperature normalized PL spectra of $(Ca_{3.95-y}Ba_y)(PO_4)_2O$: $0.05Eu^{2+}$ phosphors for an excitation wavelength of 450 nm, the emission intensity at 594nm which shifted to shorter wavelength as $Ba^{2+}/Sr^{2+}$the substituted in the lattices of Ca^{2+} ion.

In general, the electronic configuration of Eu^{2+} is $4f^7$ and $4f^65d^1$ at the ground and excited state, respectively, and the luminescence of Eu^{2+} is ascribed to the $4f^75d^1$ into $4f^75d^0$ transition which results in the broad band emission The emission wavelength of Eu^{2+} depends strongly on the structure of the host crystal through the crystal field splitting of the 5d band and the ground state for the $4f^7$ electronic configuration [17-20].

As stated above, the positions of the $4f^6d^1$ levels are much more influenced by the outer crystal field interaction than the $4f^7$ levels and highly depend on the crystalline environment around Eu^{2+} ion, so significant optical changes are expected if local structure around the Eu^{2+} center is different [7, 8]. In case of as-synthesized $Ca_{3.95-y-z}Ba_ySr_z)(PO_4)_2O:0.05Eu^{2+}$ phosphors, the environment around Eu^{2+} ions have uniform crystal structures. The unit cell volume of $Ca_4(PO_4)_2O$ is less than $Ba_4(PO_4)_2O$ and $Sr_4(PO_4)_2O$ hosts due to ionic size difference of Sr^{2+}/Ba^{2+} and Ca^{2+} ions and the ionic size of Eu^{2+} less than that of $Sr^{2+}$and Ba^{2+} ions, upon Eu^{2+} doping in to the above hosts. The is $Ba_4(PO_4)_2O$ and $Sr_4(PO_4)_2O$ less than slightly distortion than $Ca_4(PO_4)_2O$ hosts because of the size difference between Eu^{2+} and Ba^{2+} /Sr^{2+} bigger than the size of Ca^{2+} ions. Therefore, PL spectrum of the dopant Eu^{2+} ion experienced strong crystal fields (blue shift) and low symmetry (broaden) in Ca_{4-y-}

$_z$Ba$_y$Sr$_z$)(PO$_4$)$_2$O than Ca$_4$(PO$_4$)$_2$O: 0.05Eu^{2+} phosphors, due to local structure (symmetry) difference around Eu^{2+} center in the respective hosts.

When content of Ba^{2+}/Sr^{2+} ions increased from (y = 0.1 to 1.0, and z = 0.1 to 1.0) the emission peak positions gradually move toward longer wavelengths from 594 nm to 594 nm, and in addition, the FWHM of Eu^{2+} ions emission broaden from 140 nm to 210 nm (see Figure 4. 6(a)). For (Ca$_{3.95-y}$Ba$_y$)(PO$_4$)$_2$O: 0.05Eu^{2+} phosphors, the about 70 nm shift and 51 nm broadening allow highly color-tunable phosphors by changing the content of Ba^{2+}/Sr^{2+} ions [35-38].

This indicate that the lattices of (Ca$_{2.95}$Ba$_{0.50}$Sr$_{0.50}$)(PO$_4$)$_2$O host combined from an expanded Ba-O/Sr-O and contracted Ca-O bonds which create different environments around the sites of Eu^{2+} ions doped in the lattice of (Ca$_{2.95}$Ba$_{0.50}$Sr$_{0.50}$)(PO$_4$)$_2$O phosphor and cause for the blue shifts and spectral broadening of Eu^{2+} activated (Ca$_{2.95}$Ba$_{0.50}$Sr$_{0.50}$)(PO$_4$)$_2$O phosphors.

Figure 4. 7 shows the emission spectra of $Ca_{4-x}(PO_4)_2O:xEu^{2+}$ with different Eu^{2+} concentration. It can be seen from the Figure, the optimal Eu^{2+} content was about x= 0.10. When the content of Eu^{2+} ions was over x = 0.05, concentration quenching occurred and emission intensity decreased with increasing Eu^{2+} ions concentration. Moreover, emission wavelength as well as emission intensity of the $Ca_{4-x}(PO_4)_2O:xEu^{2+}$ phosphors were changed by varying the concentration of Eu^{2+} ions. As the concentration of Eu^{2+} ions in the host lattice was increased, the emission wavelength shifted slightly to a shorter wavelength. With an increase of the Eu^{2+} concentration x , the integrated emission intensity slightly increases with a breaking point $x \approx$ 0.10, which establish its higher emission efficiency.

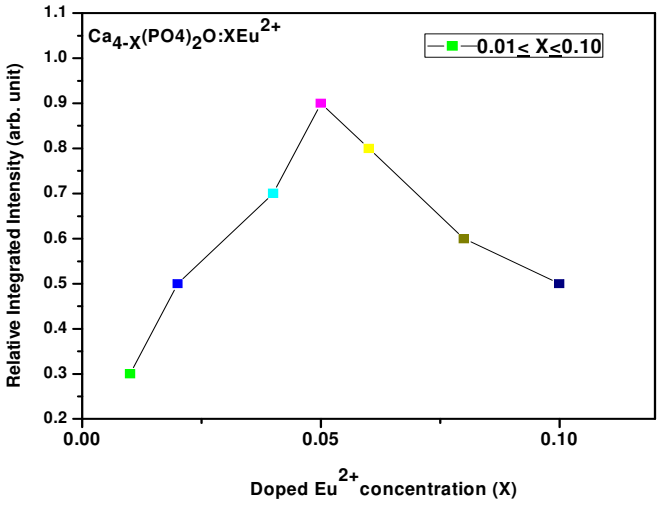

Figure 4. 7 Relative integrated emission intensity of $Ca_{4-x}(PO_4)_2O:xEu^{2+}$ with different Eu^{2+} concentration under an excitation of 450 nm.

Upon excitation at a wavelength of 450 nm, The external quantum efficiency of $(Ca_{2.95}Ba_{0.50}Sr_{0.50})(PO_4)_2O:0.05Eu^{2+}$ and $(Sr,Ba)_2SiO_4:Eu^{2+}$ well known yellow phosphor are determined to be 38.7% and 70.9%, respectively. The lower quantum efficiencies of $(Ca_{2.95}Ba_{0.50}Sr_{0.50})(PO_4)_2O:0.05Eu^{2+}$could be further enhanced by process optimization.

3.3 Application to White LEDs.

Figure 4. 8 shows photometric and colorimetric quantities of the white LEDs under the following applied currents: 20, 50, 100, 150, 200, 250, 300 and 350mA. When the applied current was 350mA, the white LED have CIE color coordinate of (0.3354, 0.3448) at a white light (Tc = 5500 K) and an excellent *Ra* of 86.The CIE color coordinates shifted towards the white light region along the Planckian locus, the value of Ra decreased from 91.6 to 86.0 and the luminous efficiency decreased from 21.5 to 16.5 lm/W as the applied current was increased. In comparison with the blue InGaN chip pumped with YAG:Ce^{3+} phosphor (Ra = 75, CCT=7756K), and $LaSr_2AlO_5$ phosphor (R_a = 85-85, CCT = 4200-5500 K) [19,20], the white LEDs in this study shows higher Ra value and lower CCT value. Therefore, the (Ca, Ba, $Sr)_4(PO_4)_2O:Eu^{2+}$ phosphors are promising for application in excellent R_a white LEDs.

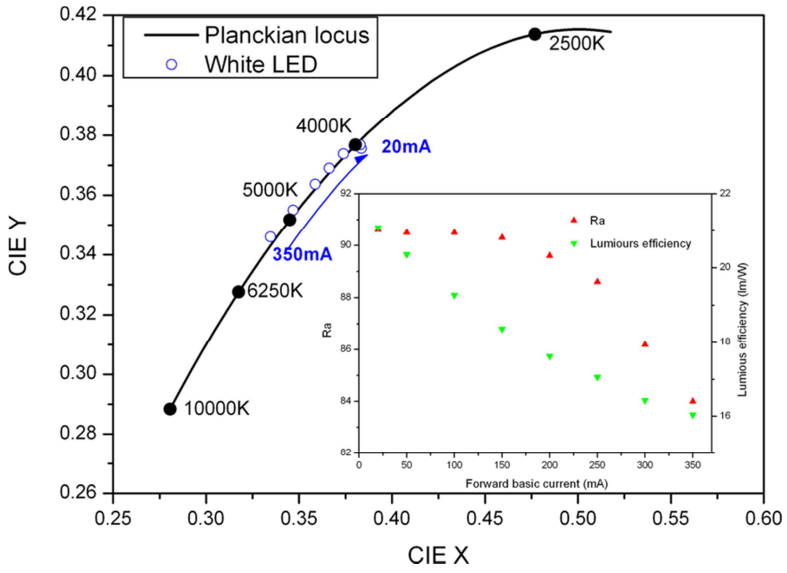

Figure 4. 8 CIE chromatic coordinates, R_a and luminous efficiency (the inset) of the white LED using $(Ca_{2.95}Ba_{0.50}Sr_{0.50})(PO_4)_2O{:}0.05Eu^{2+}$ under various applied currents. The Planckian locus line and the points corresponding to color temperatures are indicated.

5. CONCLUSIONS

In summary, a tunable red-to-yellow- emitting $Ca_{3.95-y-z}Ba_ySr_z)(PO_4)_2O:0.05Eu^{2+}$ phosphors have been reported. The excitation spectrum shows broad band excitation in the near-ultraviolet, ultraviolet and blue region, which matches well with blue chips $(Ca, Ba, Sr)_4(PO_4)_2O:Eu^{2+}$ is excitable over a broad range from 500 to 800 nm, and its emission can be adjusted from yellow to red to by changing Ba^{2+}/Sr^{2+} doping concentration. Applying $(Ca_{2.95}Ba_{0.50}Sr_{0.50})(PO_4)_2O:0.05Eu^{2+}$phosphor on blue chip, we can obtain a white LED device with high R_a of 88 and CCT value of 5450 K. With the interesting tunable emission property, $(Ca, Ba)_4(PO_4)_2O: Eu^{2+}$ phosphor has great application potential as a good color conversion material for solid state lighting.

ACKNOWLEDGEMENTS

This research was supported by School of Applied Natural Science, Adama Science and Technologu University under Eight Cycle ASTU Research Grant.

Some of the laboratory activities were done in the Department of Display Science and Engineering, Pukyong National University, Busan, 608-737, Republic of Korea

REFERENCES

1. ″LED". The American heritage science dictionary. Houghton Mifflin Company. 2005.
2. Moreno, Ivan; Sun, Ching-Cherng (2008). "Modeling the radiation pattern of LEDs". Optics Express.**16**(3): 1808–1819.
3. Thomas M. Okon; James R. Biard (2015)."The First Practical LED". EdisonTech Center. org.
4. "Cleaning Up a Broken CFL". www.epa.gov. United States Environmental Protection Agency.
5. Carlessi, F., MO Oliveira2 HO Ando Junior, J. M. Neto, A. D. Spacek, V. L. Coelho, L. Schaeffer, H. Bordon, O. E. Perrone, and A. S. Bretas. "Evaluation of Alternative Disposal and Replacement of Fluorescent Lamps". International Conference on Renewable Energies and Power Quality (ICREPQ'13).
6. Bachmann, V. Ronda, C. and Meijerink, A. **(2009)**. Chem. Mater., **21**, 2077.
7. Schubert, E. F. and Kim, J. K. **(2005).** Science, **308**, 1274.
8. Deressa, G. Park, K.W. Jeong, H.S. Lim, S.G. Kim, H.J. Jeong, Y.S. and Kim, J.S., **(2015).** J. Lumin. **161**, 347.
9. Setlur, A., Radkov, V. E Henderson, S. C. , J. Her, M. A. Srivastava, N. K., M. Kishore, N. Kumar, D. Aesram, A. Deshpande, A. Kolodin, L. Grigorov, U. Happek, **(2010)**, *Chem. Mater.*, **22**, 4076.
10. Im, W. S. Brinkley, J. Hu, A. Mikhailovsky, S. DenBaars, R. Seshadri **(2010)**. *Chem. Mater.*, **22**, , 2842.

11. Wu, Y., D. Wang, T. Chen, C. Lee, K. Chen, H. Kuo **(2011)**. *ACS Appl. Mater. Interfaces*, **3**, 3195.
12. Yu, H., D. Deng, D. Zhou, W. Yuan, Q. Zhao, Y. Hua, S. Zhao, L. Huang, S. Xu **(2013)**. *J. Mater. Chem. C*, **1**, 5577**.**
13. Zhou, X., X.Yang, Y. Wang, X. Zhao, L. Li, Q. Li **(2014)**. *Alloy. Comp.*,**608**, , 25.
14. Dorenbos, P., **(2013)**. ECS: J. Solid State Sci. Technol. **2**, R3001.
15. Zhang, Z., O. M. ten Kate, A. Delsing, E. van der Kolk, P. H. L. Notten, P. Dorenbos, J. Zhao and H. T. Hintzen. **(2012)**. J. Mat. Chem. **22,** 9813.
16. Yang, P., G.-Q. Yao, and J.-H. Lin, **(2004).** Inorg. Chem. Commun. **7**, 302.
17. Zhou, L., H. Liang, P. A. Tanner, S. Zhang, D. Hou, C. Liu, Y. Tao, Y. Huang and L Li, **(2013)** J. Mater. Chem. C, **1**, 7155.
18. Kottaisamy, M., R. Jagannathan, P. Jeyagopal, R. Rao, and R. Narayanan, **(1994)**. J. Phy. D: Appl. Phys. **27**, 2210
19. Deng, D., H. Yu, Y. Li, Y. Hua, G. Jia, S. Zhao, **(2013)**. *J. Mater. Chem. C*, **1**, 3194**.**
20. Huang, Y., H. Ding, K. Jang, E. Cho, H. Lee, M. Jayasimhadri, S.Yi, **(2008)** *J. Phys. D:Appl. Phys.*, **41**, 095110**.**
21. Harvey, E.N. A History of Luminescence: From the Earliest Times Until 1900, The American Philosophical Society, Philadelphia, (1957).
22. Needham, D.M. Machina Carnis: The biochemistry of muscular contraction in its historical development, Cambridge University Press, (1971).
23. Laverenz, H.V. An Introduction to Luminescence of Solids, Dover Publications, New York, (1968), 90.

24. Haver, O.T.C. **(1978).** J. Chem. Educ., 55, 423.
25. Stokes, G.G. **(1852)**. Phil.Trans. 142, 463.
26. Stokes, (G.G. **1853).** Phil.Trans. 143, , 385.
27. Rapp, R.C. Luminescence and the Solid State, U.S.A, 2004
28. Lakowicz J.R., Principles of Fluorescence Spectroscopy, Kluwer Academic/Plenum Publishers, New York, 2006
29. Meyer, F., H. Spanner, and E. Germer, **(1927)** "Metal vapor lamp," US Patent 2.182, , 732.
30. Inman, G. **(1936)** "Electric discharge lamp," US Patent 2.259, 040.
31. Son, Y.W., M.L. Cohen, and S.G. Louie, **(2006).** Phys. Rev. Lett., 97, 216803.
32. Kitai, A.: Luminescence Materials and application, Wiley, New York, **2008**.
33. Heiman, D. Photoluminescence Spectroscopy, Northeastern University, **2004**
34. Hoffmann, R. Solids and Surfaces, a Chemist's View of Bonding in Extended Structures, VCH, Weinheim, **1988**.
35. Ronda, C.R. Luminescence. From Theory to Applications, VCH, Weinheim, **2008**.
36. Sommerdijk,. J. L., A. Bril, and A. W. de Jager," **(1974)**, J. Lumin., 8, 341.
37. Piper, W. W. J. A. de Luca, and F. S. Ham, **(1974)** J. Lumin., 8, , 344.
38. Wegh, R. T., H. Donker, K. D. Oskam, and A. Meijerink, **(1999).** Science, 288, 663.
39. Oskam, K. D., R. T. Wegh, H. Donker, E. V. D. van Loef, and A. Meijerink, **(2000)**. J. Alloys Compds., 421, 300.